



**Fermi National Accelerator Laboratory**

**FERMILAB-Pub-97/092**

**Evaluation of Candidate Photomultiplier Tubes for the Upgrade of  
the CDF End Plug Calorimeter**

W. Koska et al.

*Fermi National Accelerator Laboratory  
P.O. Box 500, Batavia, Illinois 60510*

May 1997

Submitted to *Nuclear Instruments and Methods A*

## **Disclaimer**

*This report was prepared as an account of work sponsored by an agency of the United States Government. Neither the United States Government nor any agency thereof, nor any of their employees, makes any warranty, expressed or implied, or assumes any legal liability or responsibility for the accuracy, completeness, or usefulness of any information, apparatus, product, or process disclosed, or represents that its use would not infringe privately owned rights. Reference herein to any specific commercial product, process, or service by trade name, trademark, manufacturer, or otherwise, does not necessarily constitute or imply its endorsement, recommendation, or favoring by the United States Government or any agency thereof. The views and opinions of authors expressed herein do not necessarily state or reflect those of the United States Government or any agency thereof.*

## **Distribution**

*Approved for public release; further dissemination unlimited.*

**Evaluation of Candidate Photomultiplier Tubes  
for the  
Upgrade of the CDF End Plug Calorimeter**

W. Koska, S. W. Delchamps, W. Kinney,  
D. C. Lewis, P. J. Limon, A. Ronzhin, J. Strait  
Fermi National Accelerator Laboratory  
P.O. Box 500, Batavia, IL 60510

I. Fiori  
INFN and Dipartimento di Fisica  
University of Bologna, Bologna, Italy

M. Gallinaro  
INFN and Dipartimento di Fisica  
University of Padova, Padova, Italy

Y. Pischalnikov, Q. Shen  
Department of Physics  
Purdue University, West Lafayette, IN 47904

**Abstract**

The Collider Detector at Fermilab is upgrading its end plug calorimeter from a gas detector system to one using scintillating tiles read out through wavelength shifting fibers. This upgrade is required to take advantage of the increase in luminosity which the Tevatron will provide in the future. The tile-fiber calorimeter, which is longitudinally segmented into electromagnetic and hadronic sections, will be read out through 1,824 photomultiplier tubes. The performance requirements of the calorimeter demand that the PMTs have good response to light in the 500 nm region, provide adequate amplification for signals from minimum ionizing particles, provide linear response for peak anode currents up to 25 mA at a gain of  $5 \times 10^4$ , and fit into the restricted space at the rear of the plugs. For convenience, we also desire a single PMT and base combination be used for the electromagnetic and hadron calorimeters even though the required gains in these sections differ by a factor of 10. This paper describes the evaluation process used to determine the adequacy of the commercially available PMTs which appeared to meet our performance requirements.

## Introduction

The Collider Detector at Fermilab (CDF)<sup>1</sup> is upgrading its end plug calorimeter from a gas detector system<sup>2</sup> to one using scintillating tiles read out through wavelength shifting (WLS) fibers<sup>3</sup>. This tile-fiber calorimeter is longitudinally segmented into electromagnetic (EM) and hadronic (HAD) sections which will be read out through 1,824 photomultiplier tubes (PMTs). To optimize calorimeter resolution we wanted a PMT with high quantum efficiency for light emitted by WLS fibers. For convenience, we desire a single PMT type for both the EM and HAD sections of the calorimeters even though the inherent difference between electromagnetic and hadronic showers requires those PMTs that service the HAD calorimeter to operate at a gain approximately ten times greater than those servicing the EM calorimeter. This, in combination with uncertainty concerning the final light output per minimum ionizing particle the tiles would be able to achieve, the eventual luminosity of the Tevatron and the final electronics design, forced us to specify a gain regime ranging from  $1 \times 10^4$  to  $1 \times 10^6$ . We desire linear PMT response for input signals ranging from approximately 50 photoelectrons (from minimum ionizing particles) to  $1.5 \times 10^5$  (EM) and  $1.2 \times 10^4$  (HAD) photoelectrons, corresponding to 400 GeV electrons and 600 GeV hadronic jets, respectively. The phototubes are also required to fit into the restricted space at the rear of the plug calorimeters. Furthermore, each PMT must accept the light from 24 fibers, of diameter 1.0 mm, arranged in a well-defined matrix such that individual fibers can be masked if necessary to compensate for variations in individual tile response. The calorimeters will be calibrated with a radioactive source, implying that PMT dark currents must be low (under 5 nA) in order to reduce calibration noise. The PMTs must also be capable of surviving an integrated anode charge approaching 100 Coulombs, which, for the inner calorimeter towers would correspond to approximately three years of operation at a luminosity of  $10^{32} \text{ cm}^{-2}\text{-s}^{-1}$ . Finally, the overall system must have a low spontaneous discharge rate to avoid producing spurious PMT signals great enough to trigger the data acquisition system of CDF.

These requirements limited the search for an acceptable PMT to those with: 1) a green extended photocathode to provide a good match to the spectrum of light emitted from the WLS fiber, 2) eight or ten stages to provide the required gain range, 3) an outer diameter of less than 20 mm in order to fit within the limited space and 4) an active photocathode diameter greater than 14 mm in order to accept all the fibers. PMTs that appeared to meet most of these requirements were the Burle C83012E (10 stages), the Hamamatsu R4125 (10 stages), the Philips XP1901 (10 stages), the Philips XP1981 (8 stages) and the Thorn EMI D919B (10 stages). Of these, the C83012E uses a wire anode that restricts its linear range to less than 1 mA peak current, which is well below our requirements and disqualified it from further consideration.

Candidate PMTs were evaluated with regard to the following performance characteristics: 1) gain versus voltage, 2) dark current versus voltage, 3) relative quantum efficiency, 4) uniformity of photocathode response, 5) linearity of response to various input signals, and 6) stability. An accelerated lifetime test was also performed on two of the types of tubes. In addition to reporting on these studies, we will discuss the mechanical assembly in which the PMTs will be housed and the spontaneous discharge rate of the system.

## The Test and Data Acquisition System

Several test systems were constructed so that PMT evaluations could be performed in a timely fashion. A block diagram of a typical test system is shown in figure 1). An Intel 486 based PC<sup>4</sup> was used to control voltage settings of the tubes, adjust excitation

sources, acquire data and perform simple data reduction algorithms. The primary excitation

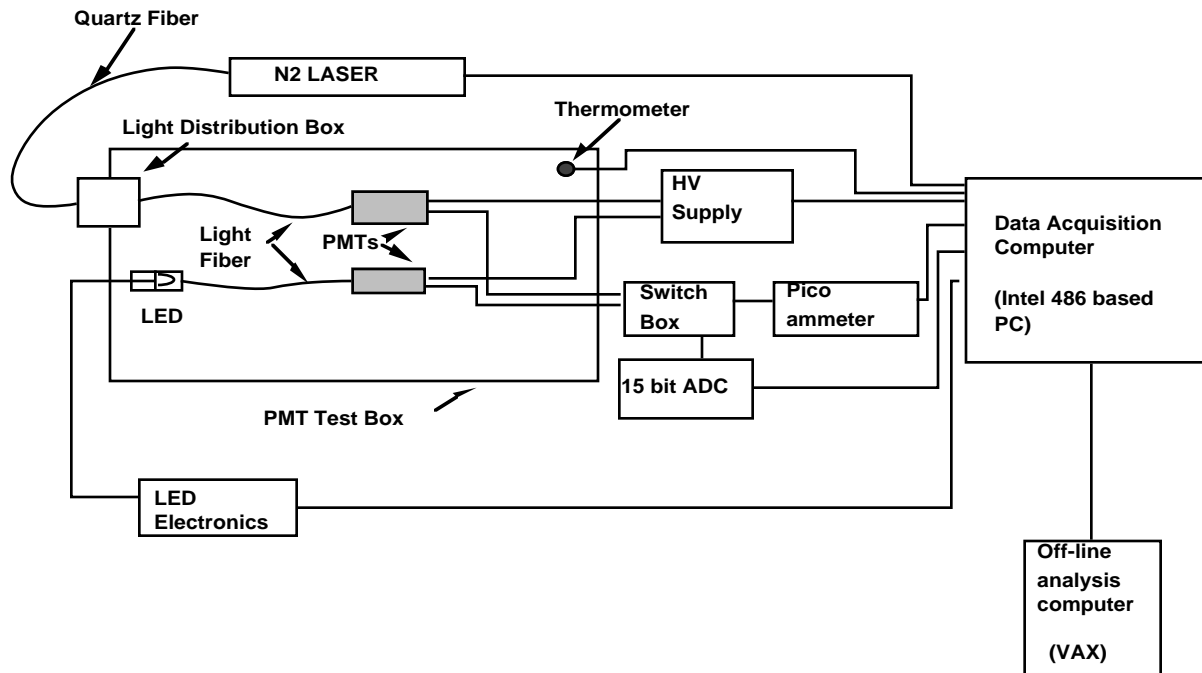


Figure 1) Block diagram of a photomultiplier tube test system. The data acquisition computer controls the high voltage, LED amplitude and pulse frequency, data acquisition rate, data acquisition mode (i.e. picoammeter or ADC readout) and measurement sequence. Preliminary analysis is done on-line and the results are displayed for test monitoring purposes. Recorded data are later moved to the VAX for further analysis.

source for determination of PMT gain was a red LED<sup>5</sup>, which could be pulsed at the limit of the data acquisition system, about 128 Hz. A driver card was built that allowed the data acquisition computer to control the current flowing through the LED in both pulse and steady state mode, allowing control of the pulse rate and the amplitude of the emitted light. This versatility allowed measurements to be easily made over the full range of the PMT gain. In pulse mode the LED was excited such that pulses were approximately 60 ns full width at their base. Attempting to obtain shorter pulses led to non-uniform LED light output. We found that the LED required approximately ten minutes of pulsed operation before stable light amplitudes were attained.

A computer controlled relay was used to route the PMT output to either a picoammeter<sup>6</sup> for steady state current measurements, or a 15 bit ADC<sup>7</sup> (~0.033 pC/count resolution) for pulse measurements. One test system was built to accommodate 24 PMTs so that long term stability tests could be performed on a reasonably large sample of tubes simultaneously. The primary excitation source for this stand was a pulsed nitrogen laser<sup>8</sup> which emitted UV light at 337 nm. The laser light was transported by a quartz fiber to the test chamber, where it was used to excite a plastic scintillator. Light from the scintillator was collected by wavelength shifting fibers and was transported to the PMTs by clear fibers which were spliced to the WLS fibers. Linearity tests were performed on a system developed by the Fermilab Physics Department.

### Determination of Gain and Dark Current versus Voltage

The gain of a PMT was determined by measuring the distribution of its response to some number of fixed amplitude pulses (typically 10,000) from a red LED. The LED pulse width was approximately 60 ns full width at its base and the pulse rate was 128 Hz. A

typical gain measurement took about 80 seconds. The gain may be related to the mean,  $\mu$ , and variance,  $\sigma^2$ , of the response distribution through the relation <sup>9</sup>:

$$1) \quad G = \frac{A}{eF_n} \times \frac{\sigma^2}{\mu}$$

where A is the charge per ADC count, e is the electron charge and  $F_n$  is a factor that is a function of the statistical nature of the amplification of the first few dynode stages and, for the PMT's considered, is typically in the range 1.1 to 1.2 for gains greater than  $10^5$ . The procedure used for determining gain consisted of measuring  $\mu$  and  $\sigma^2$  at increments of 100 volts in the range from 700 V to 1500 V. Equation 1 was used to calculate the gain,  $G_S$ , at 1100 volts, with  $F_n$  set equal to 1. This produced a gain measurement which had a statistical uncertainty of about 1.5% and a systematic underestimate of 10-20% (i.e. absolute gain is known only to 20%, but variations in the gain of a PMT can be monitored at the 2% level).

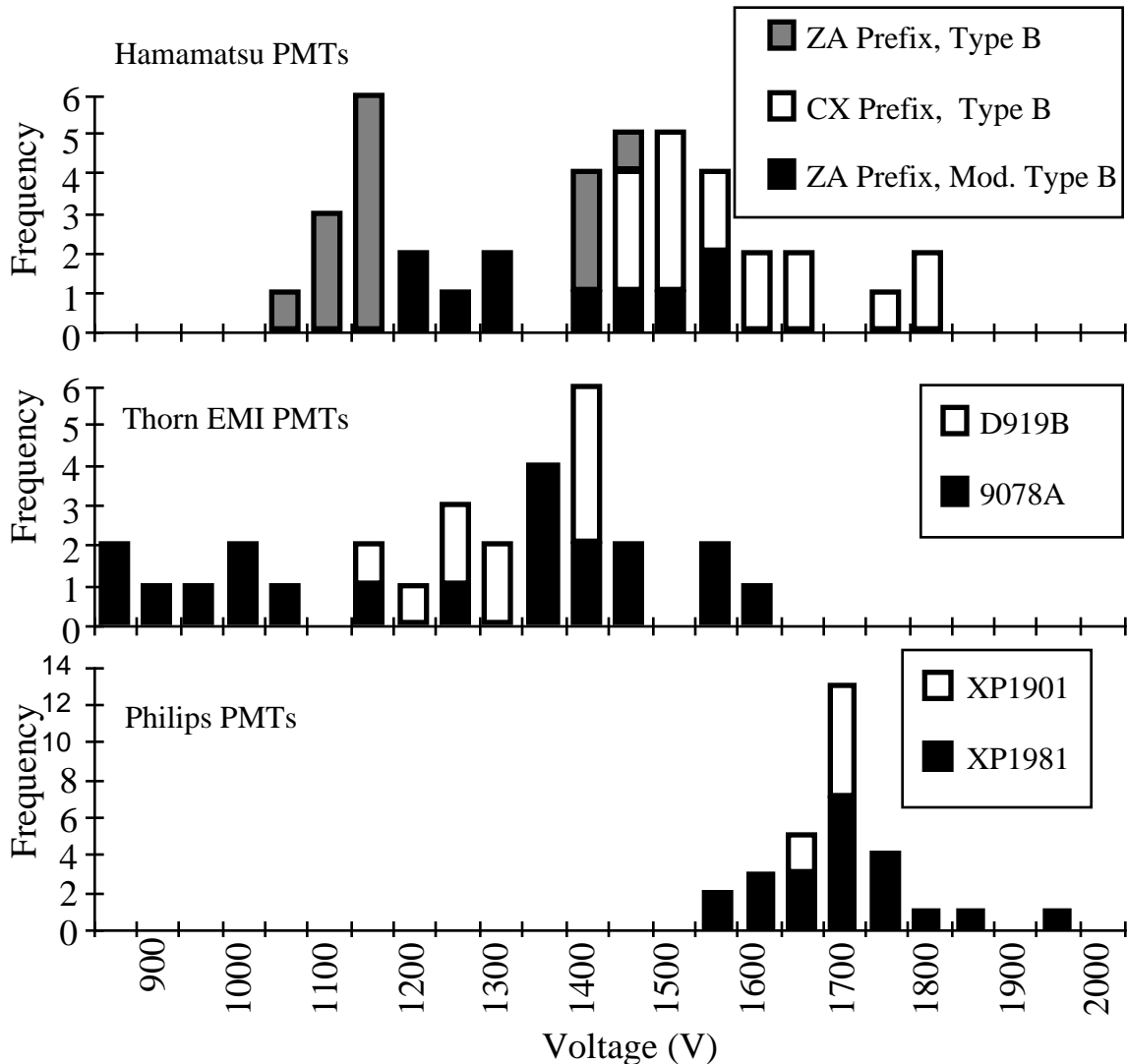


Figure 2) Distributions of voltage at which a gain of  $1 \times 10^6$  is achieved for candidate PMTs.

Using this method to determine gains at lower voltages results in a larger systematic error since  $F_n$  increases as voltage (and therefore gain) decreases. Tube gains at other voltages were determined by relating the mean values of the response distributions at these voltages to the mean measured at 1100 V. A linear fit was made to the plot of  $\log G$  versus  $\log V$ , and the fit parameters were used to determine the voltage to achieve any gain to within 20%.

Figure 2) displays histograms of the required voltage to produce a gain of  $1 \times 10^6$  for several tube types, as determined using the procedure described above. The dividers used in these tests were tapered resistive chains with capacitors across the last 3 or 4 dynode stages. The upper plot shows the distribution for the R4125 PMTs tested. We received R4125 PMTs from Hamamatsu which had serial numbers prefixed with a CX or ZA and permanently attached bases. A third set of R4125s were tested with voltage divider networks recommended by the vendor (modified type B) for improved linearity at low gain. A divider optimized for linearity will lower the gain with respect to voltage. Note that this histogram indicates that the CX prefixed tubes have lower average gain than the ZA tubes, even those with dividers optimized for linearity. The middle plot shows the distribution for 20 Thorn EMI 9078A (the counterpart of the D919B without a green extended photocathode) and 10 D919B PMTs. The bottom plot is the distribution for the Philips XP1981 (8 stage) and XP1901 (ten stage) PMTs. These tubes tended to be lower in gain than those from the other vendors. This is expected for the 8 stage PMTs, and since the specification for the XP1901 called for good linearity, these tubes were probably selected to be low gain in order to improve the linearity of their response. All tube types were able to reach gains of  $1 \times 10^6$  without exceeding their maximum operating voltages.

The dark current of the PMTs was determined at a sequence of voltages using the picoammeter. All tube types met our requirements of less than 5 nA dark current at a gain of  $5 \times 10^5$  at 20°C.

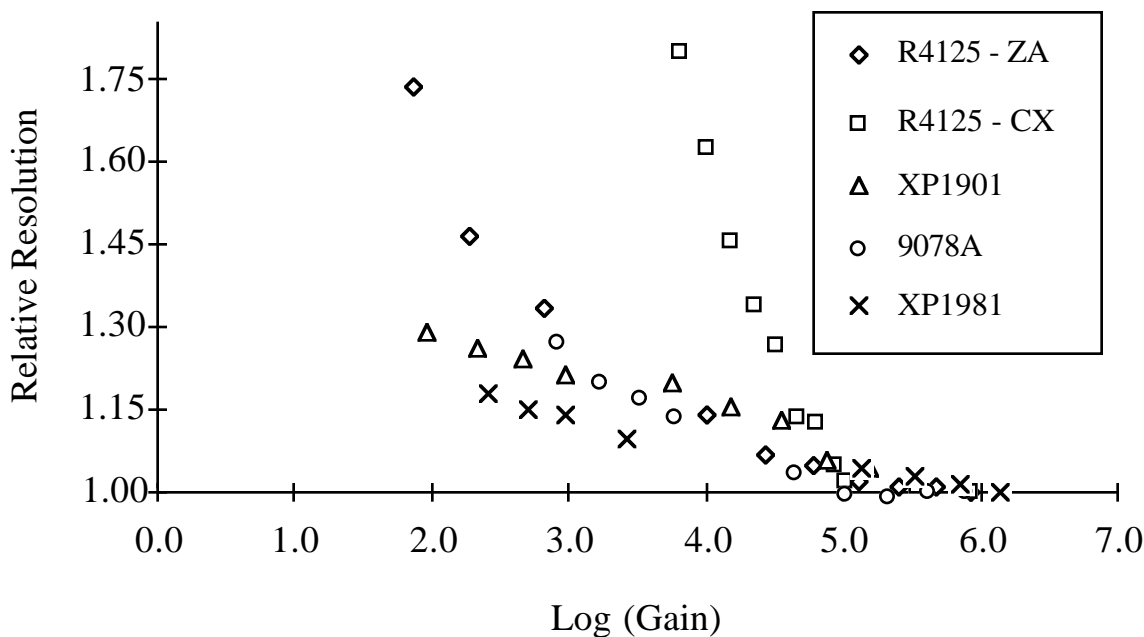


Figure 3) Relative pulse height resolution, normalized at  $G = 10^6$ .

The pulse height resolution (PHR) of a PMT, which we define as  $\sigma/\mu$ , is related to  $F_n$  through:

$$2) \quad PHR = \frac{\sigma}{\mu} = \frac{\sqrt{F_n}}{\sqrt{n_{pe}}}$$

where  $n_{pe}$  is the number of photoelectrons produced at the photocathode. It can be shown that  $F_n$  increases as PMT gain is reduced<sup>10</sup>. Since the PMTs at large pseudorapidity ( $\eta$ ) in the plug electromagnetic calorimeter may have to operate at gains of about  $1 \times 10^4$  to limit the average anode currents due to backgrounds from low momentum transfer interactions, we were concerned that the PHR might contribute significantly to the calorimeter resolution. The PHR relative to the resolution at a gain of about  $1 \times 10^6$  was measured for candidate tubes. Typical results of these measurements are shown in figure 3). The degradation in resolution was comparable for all tube types except Hamamatsu R4125 PMTs which had serial numbers prefixed with CX. These tubes, which had the worst PHR, also exhibited low gains. The combination of these two results leads us to suspect that the first stage amplification in these tubes is low. All other PMTs exhibited acceptable resolution as a function of gain.

### Relative Quantum Efficiency

The PMTs are required to have high quantum efficiency in the wavelength region around 500 nm. A typical spectral distribution for light emitted by WLS fiber<sup>11</sup> is shown in figure 4), along with typical quantum efficiency curves for regular bialkali and green extended PMTs. From the convolution of the spectral distribution with the quantum efficiency curves, we expect the signal from a green extended PMT to be about 40% greater than that from a regular bialkali PMT for light produced by WLS fiber. We compared the efficiency of green extended Hamamatsu R580-17 PMTs having plano-convex photocathodes with older R580 PMTs (non green extended) having plano-plano photocathodes and found them to be about 50% more efficient, consistent with expectation.

Photomultiplier tube relative efficiency was determined by measuring response to light pulses produced by a tile-fiber combination typical of those to be used in the calorimeter, thus assuring that the correct light spectrum was sampled. The tile was placed within a scintillating paddle telescope, which provided the data acquisition trigger when  $\beta$  particles from an approximately 2 mC  $^{106}\text{Ru}$  source passed through both counters and the tile. The light collected from the tile by the fiber was coupled to a PMT through a 10.5 mm x 10.5 mm x 45 mm light mixer similar to that which will be used in the calorimeter. This limited our measurement to the region of the photocathode that will be used in the detector. The mixer was permanently mounted in a spring loaded fixture. The PMT to be tested was mounted in a magnetic shield in a holder riding on a screw slide. After installation, the screw slide was turned until there was positive pressure exerted by the tube on the mixer, as evidenced by motion of the mixer-holder springs. This virtually guaranteed uniform contact between mixer and PMT. Results obtained with this fixture were more consistent than those obtained by using optical grease between the mixer and PMT.

The output of the PMT was coupled to an ADC through a low noise amplifier<sup>12</sup> with a charge gain of approximately 630. PMTs were run at gains of approximately  $10^5$ , so the total gain of the system was approximately  $6 \times 10^7$ . Relative efficiency was determined by counting the number of telescope triggers,  $N_O$ , that did not have corresponding signals in the PMT under test, so that the ADC output was close to pedestal,

the output for zero input. The system was adjusted so that PMTs produced an average of about three photoelectrons for a  $\beta$  particle traversal of the scintillator. This value was selected because much larger values made the zero peak difficult to resolve and there began to be significant contributions from accidental triggers initiated by  $^{106}\text{Ru}$  decays involving gamma rays. For an average signal of three photoelectrons, the zero peak was readily separated from the single photoelectron peak in the digitized PMT response distribution, as is shown in figure 5). The figure of merit for PMT efficiency that we used was the logarithm of the ratio of PMT zero counts,  $N_0$ , to the total number of triggers,  $N_t$ :

$$3) \quad Q = \ln \left( \frac{N_0}{N_t} \right).$$

The parameter Q directly measures the efficiency of interest: the probability that a photon incident on the photocathode yields a signal at the anode. It measures the product of the photocathode quantum efficiency, the collection efficiency and amplification efficiency. Q is nearly equal to the average number of pe's produced by the photocathode if the incident photon signal follows a Poisson distribution, the first dynode collection efficiency is approximately 1, and the first stage gain is large ( $\geq 5$ ).

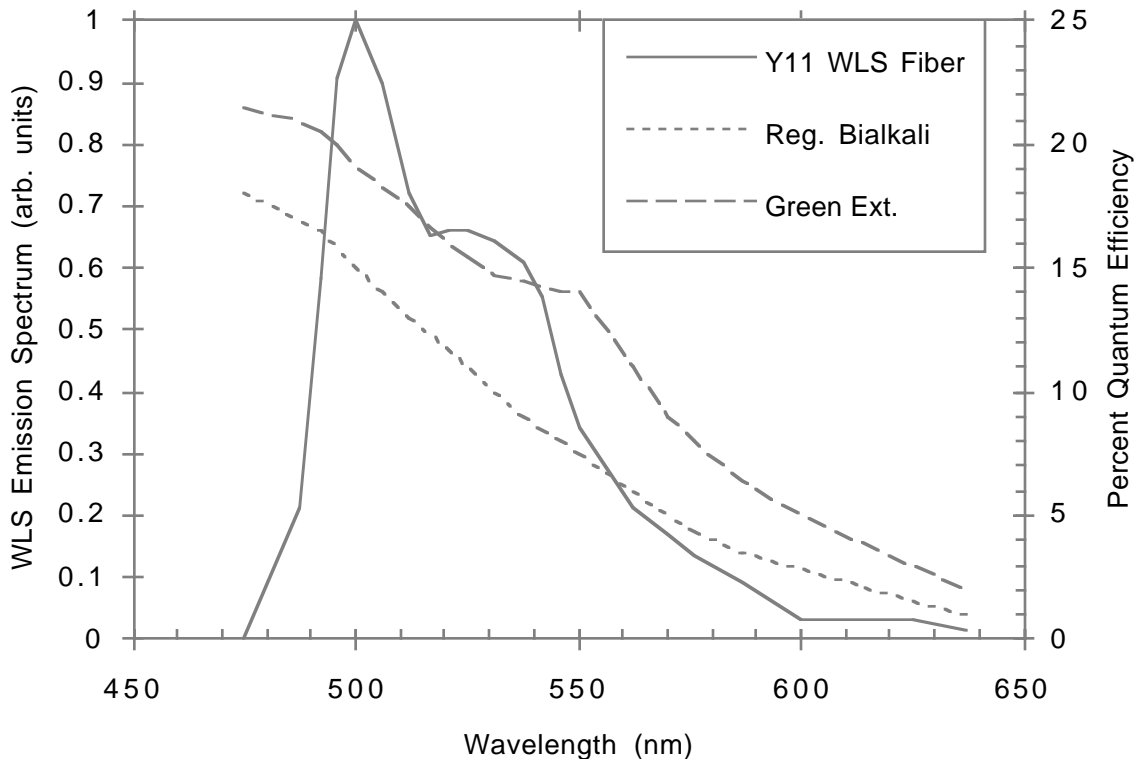


Figure 4) Comparison of quantum efficiencies of regular bialkali and green extended bialkali photocathodes. The light spectrum of the Y11-doped wavelength shifting fiber which will be used in the calorimeter is also shown.

The number of background-subtracted zero counts is determined by fitting a Gaussian function to the pedestal plus a linear function to the first approximately 15 ADC bins above the pedestal, with the constraint that the linear function pass through the horizontal axis at the mean of the Gaussian. It is corroborated by summing the number of events in the zero peak, up to three standard deviations above the gaussian mean value, and subtracting the integral of the fitted linear function over this range. From errors returned for the fit parameters by the fitting routine and by repeated measurements of a single PMT, we estimate that the uncertainty on the relative efficiency measured in this way is approximately 3%. The results of measurements made on candidate PMTs are shown in figure 6). The green extended Philips and Thorn EMI tubes exhibited comparable efficiencies, while the Hamamatsu R4125's appeared to be about 20% more efficient on average. We compared our measured relative efficiencies with the cathode luminous sensitivities and quantum efficiencies at 520 nm supplied by the vendors. We found good correlation with the data on luminous sensitivity and QE supplied by Hamamatsu for 10 PMTs. However we found poor correlation with the data supplied by Philips and Thorn EMI. We believe this is related to the photocathode uniformity, and this issue will be discussed below.

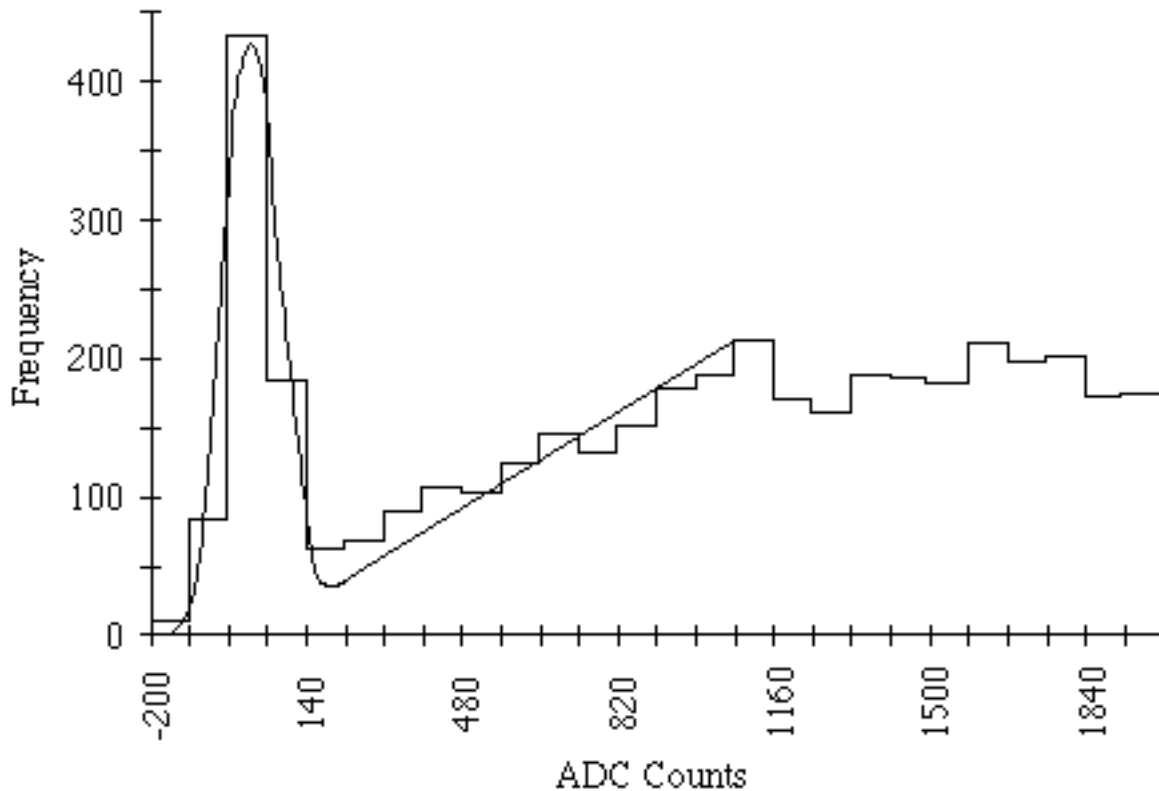


Figure 5) Typical response of a PMT to signals generated in a scintillating tile by a  $^{106}\text{Ru}$   $\beta$  source. The separation between the zero peak and the single photoelectron signal is well-defined. The fit to the data shown is illustrative of that used to determine the number of entries in the zero peak, from which the relative efficiency of the PMT is determined.

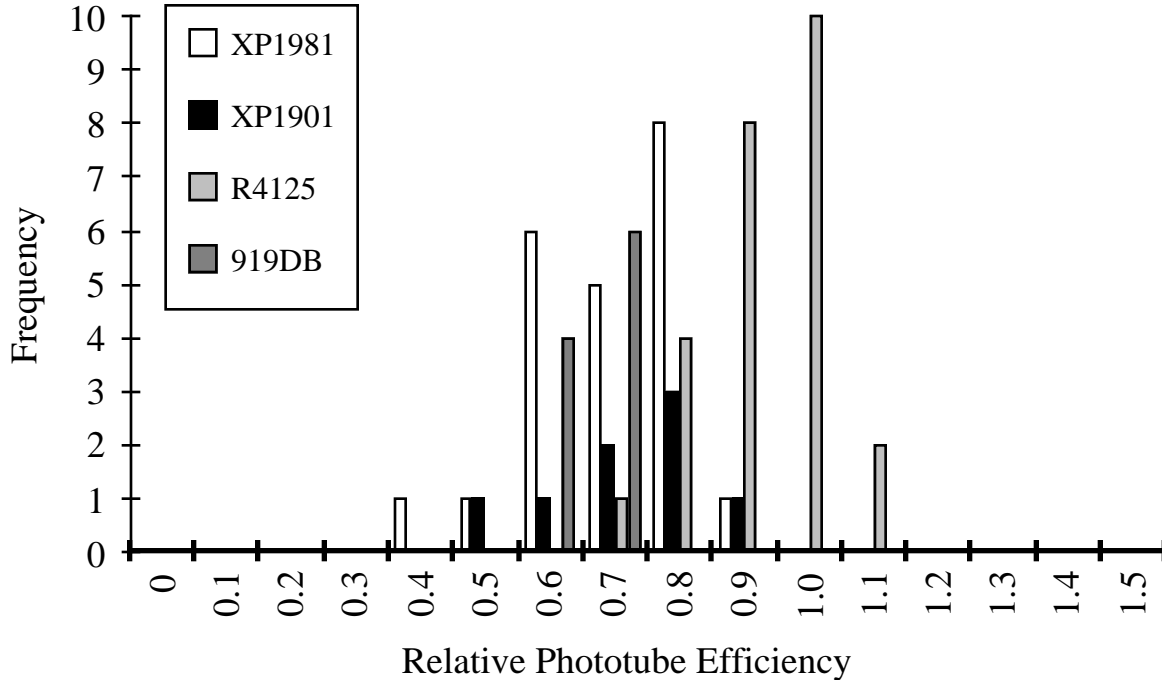


Figure 6) Relative quantum efficiency times collection efficiency for our candidate PMT types.

In addition to the  $\beta$  source measurements, we also determined relative efficiencies using the laser light source. We obtained a good correlation with the  $\beta$  source data using this method, although it is more difficult to control the systematic uncertainties. We will eventually use this method to determine efficiencies on our production PMTs, but will continue to measure a subsample using the source and tile technique.

### Photocathode Uniformity

Since sharp variations in the response of a photocathode across its surface could be indicative of manufacturing problems, a map of the response for a sample of at least two PMTs of each candidate type was made. This was done by scanning a 1 mm fiber, illuminated by a green LED operating as a steady state light source, across the face of the tube in 1 mm steps<sup>13</sup>. The LED intensity was adjusted so that the PMT produced a channel count of about 200 for an ADC with sensitivity of 0.25 pC/count and an integration gate of 700 ns. This implies an average current of about 70  $\mu$ A, well below the PMT maximum rated value of 100  $\mu$ A. The response of the tube was determined at each fiber position by averaging 100 samples. Figure 7) shows a typical response distribution, (normalized in each case to the maximum response position), for a Hamamatsu R4125, a Philips XP1981, and a Thorn EMI D919B. The R4125 appears to be uniform to within 20% over a central region approximately 10 mm in diameter. The XP1981 showed a region of reduced sensitivity near the center of its active area, relative to the perimeter, in several tubes that were measured. This observation was confirmed in measurements which used lower intensity light to eliminate the possibility it was due to a saturation effect. It is conjectured that this behavior is the result of poor collection efficiency at the first dynode, possibly due to improper spacing between cathode and dynode<sup>14</sup>. The Thorn EMI tubes

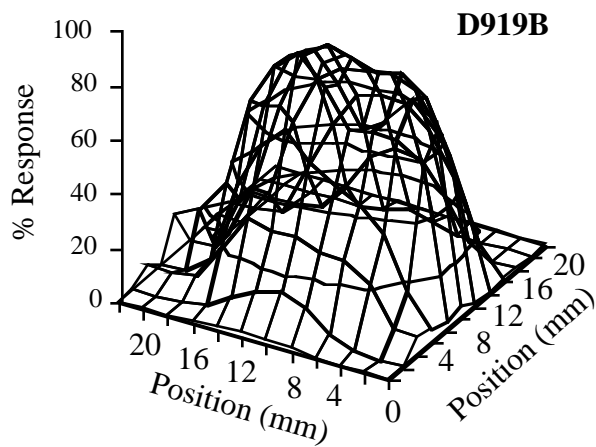
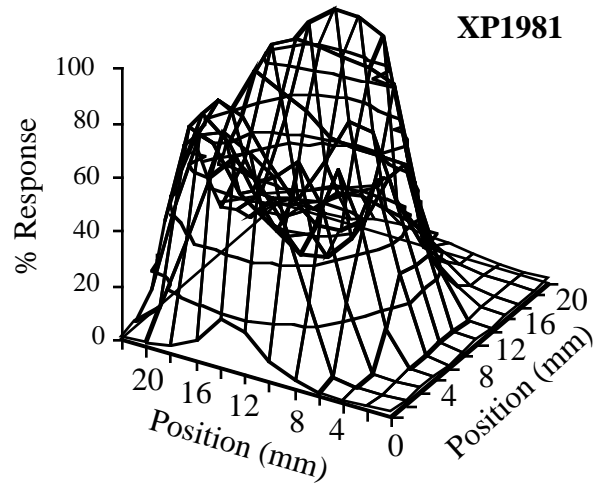
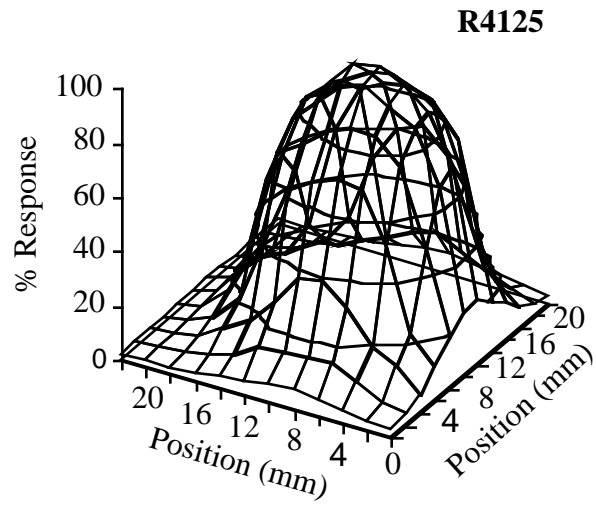


Figure 7) Comparison of spatial variations in photocathode response of candidate PMTs.

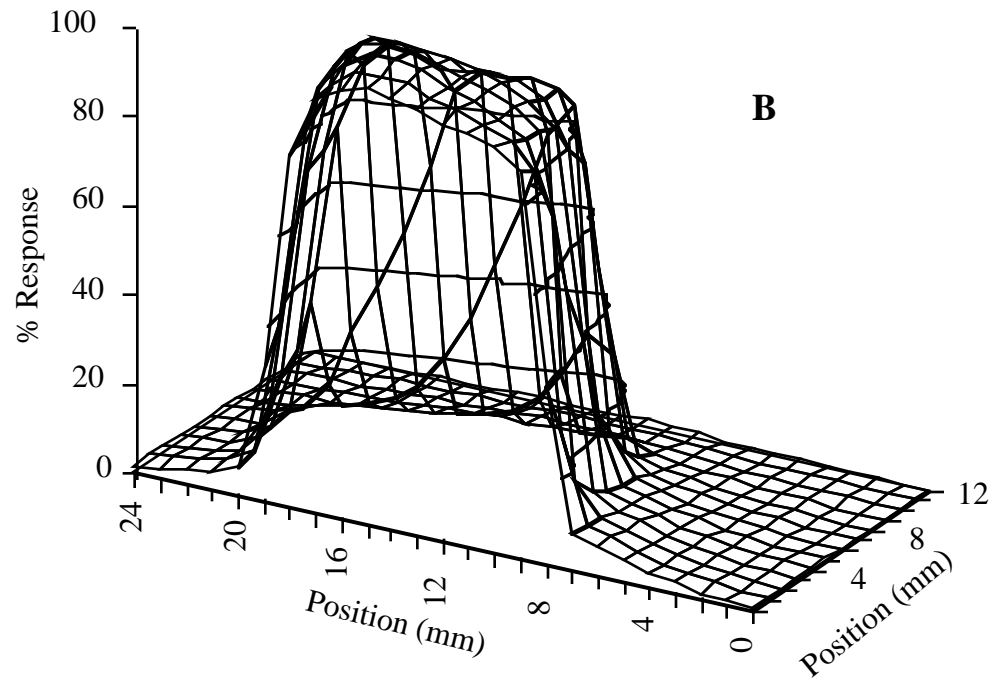
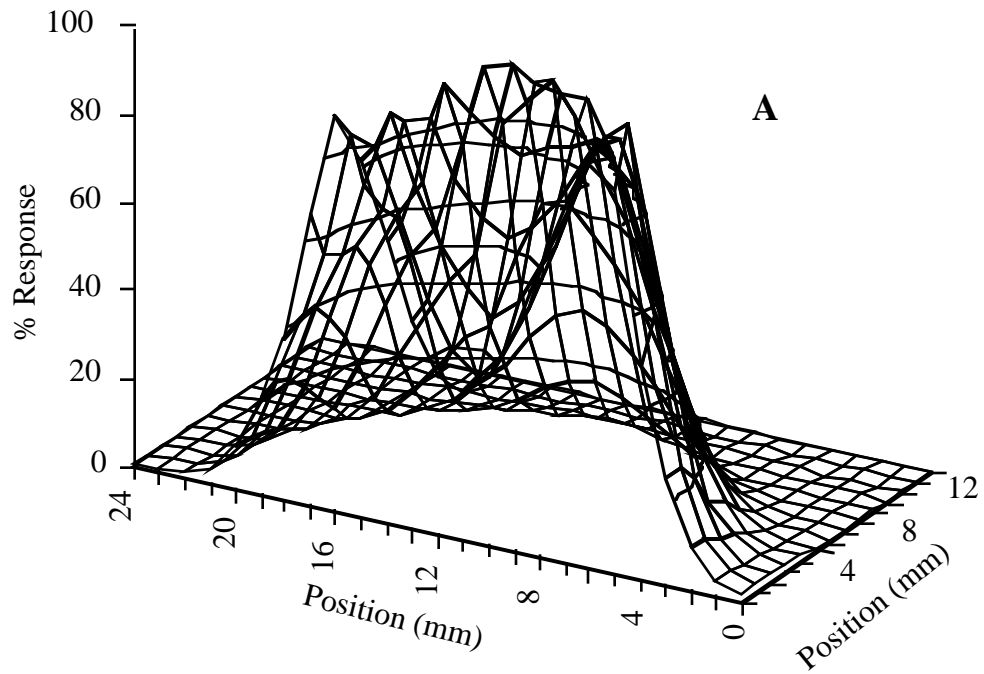


Figure 8) The upper figure shows the response map for a cross section of a PMT (with attached light mixer) to light emitted from a 1 mm fiber but restricted to a pencil beam by an extension tube. The region of very low response was due to the placement of a neutral density filter at that location. The lower figure is another scan of the same tube, but with the light allowed to exit from the fiber at its natural angle. The region of low response is negligible, indicating that the light is being properly mixed.

showed a reasonably flat response with variations on the order of 40% over the active area.

We believe that the poor correlation between our measurement of quantum efficiency and Philips's determination of cathode luminous sensitivity is related to the low response near the center of the photocathode for the Philips PMTs. Our measurement of efficiency uses a light mixer centered on the PMT, while the Philips measurement illuminates the entire photocathode and measures the current drawn from it as if it were operating as a photodiode. Since our measurement of PMT efficiency is restricted to the central region of the photocathode and includes both quantum and collection efficiencies and Philip's measurement is over the entire photocathode and is for the quantum efficiency only, it is reasonable to expect that the two techniques might yield different relative efficiency values. This underscores two points: First, if the aperture of the PMT used in an application is less than the effective cathode area, the vendor supplied cathode luminous sensitivity may not correlate well with the observed effective efficiency of the tube. Second, a discrepancy between the cathode luminous sensitivity and the relative efficiency measurement obtained using the technique outlined above may indicate a problem with cathode uniformity or collection efficiency.

The effects of moderate non-uniformities of the photocathode will be eliminated in our application by using a square light mixer. The effectiveness of a mixer with dimensions 10.5 mm x 10.5 mm x 45 mm is shown in figure 8). The upper figure shows a scan of an R4125 PMT through a mixer which had a 1 mm diameter neutral density filter (NDF) placed between the mixer and the PMT. The fiber had a 5 mm long collimator placed on its end which restricted the light cone to  $\pm 7^\circ$ , nullifying the light mixing capability of the mixer. The effect of the NDF is clearly seen in this plot; due to the NDF the response near the center of the mixer is about 60% lower than the response near the edge. The lower plot shows a scan of the same setup after the collimator has been removed. The low response due to the NDF is no longer seen and the response across about 9 mm of the mixer (the maximum we should expect considering the fiber and step size of the scanner) is flat to within  $\pm 10\%$ . This indicates that the light is being properly mixed. From the results of this experiment we believe that the mixer as designed will adequately compensate for photocathode response variations. Additional tests, with mixers epoxied<sup>15</sup> to the faces of PMTs which meet our specifications for cathode uniformity, indicate that they flatten the response to  $\pm 1\%$ . However, one drawback to the mixer is that it provides a means by which Cerenkov light generated by cosmic rays can produce spurious PMT signals. This will be discussed in more detail below.

## **Linearity of Response**

The PMTs are required to respond in a linear manner for signals ranging from those produced by minimum ionizing particles to those produced by 400 GeV electromagnetic showers or 600 GeV hadronic showers. This implies a dynamic range of 1600 : 1. The value of the current at the peak of the anode pulse at which the response deviated from linearity by more than 2% was determined for a candidate PMT by measuring its response to flashes of green light delivered to the tube by way of a wavelength shifting fiber that viewed a scintillator which was excited by a pulsed nitrogen UV laser. The PMT responses to the laser flashes were normalized to the output of a PIN diode exposed to the scintillator, to compensate for pulse to pulse variations in laser output which could be as large as 10%. Measurements were made at gains of  $10^4$ ,  $5 \times 10^4$ ,  $10^5$  and  $5 \times 10^5$  in order to span the range over which the tubes are expected to operate.

To measure linearity, the PIN diode and PMT responses are recorded for several thousand flashes of the laser while the laser light passes through a rotating filter wheel with optical density logarithmically distributed between 0.1 and 2.0 (~90% to ~1% transmission). A linear least square fit is made to the data below 90% of the maximum PIN

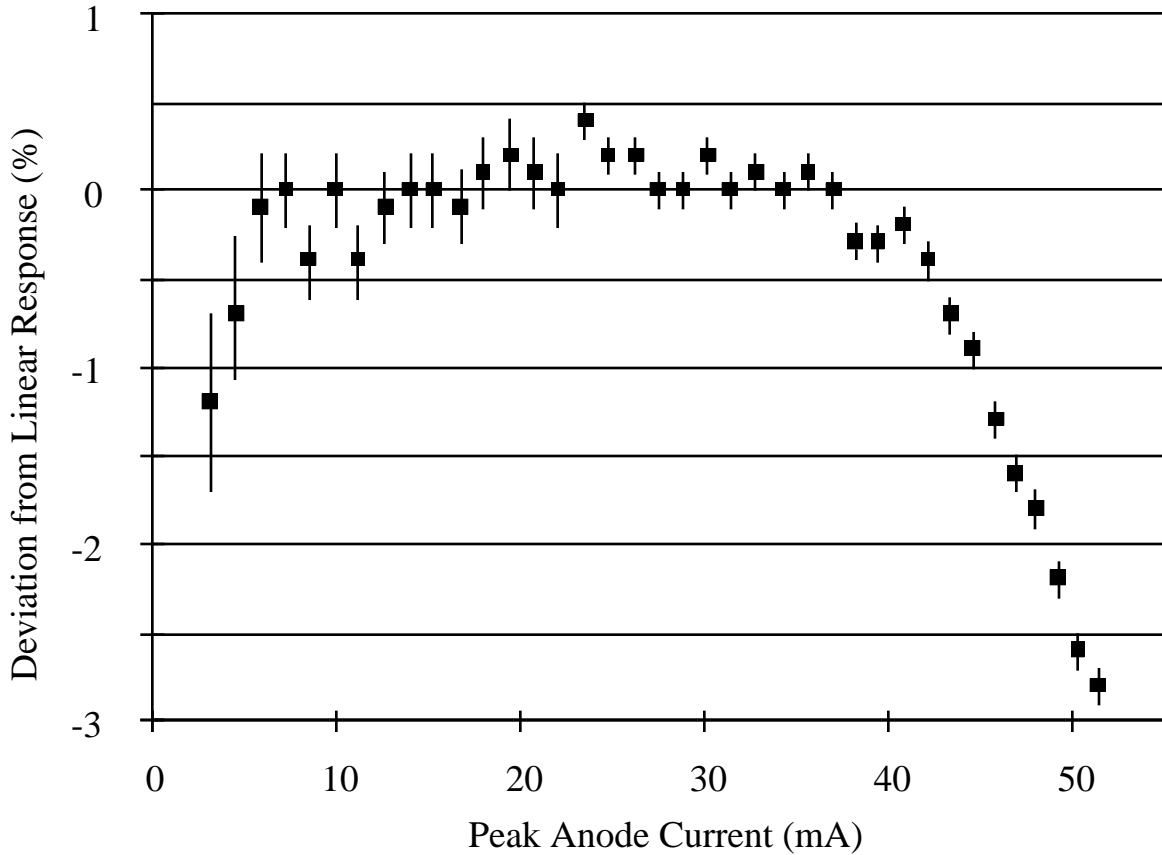


Figure 9) Result of a typical linearity measurement. The response of this PMT departs from linearity by 2% at about 50 mA peak anode current.

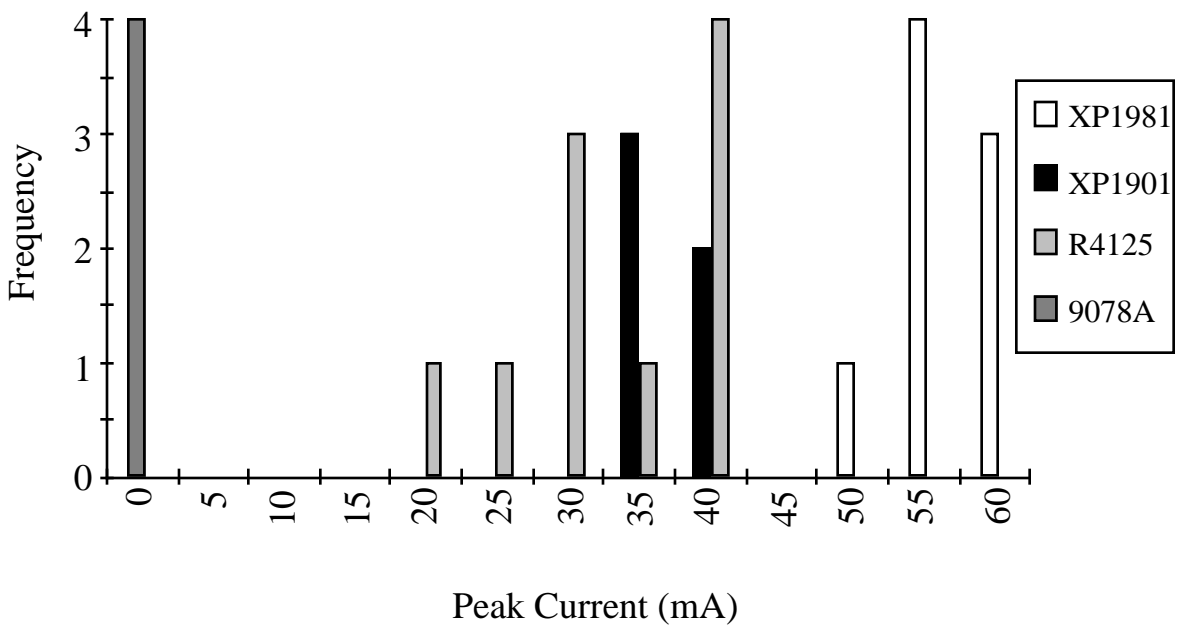


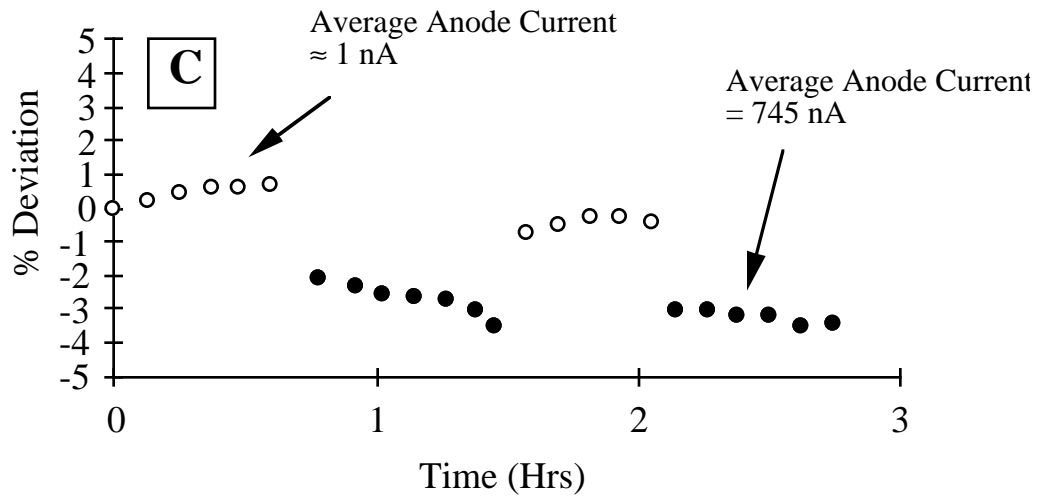
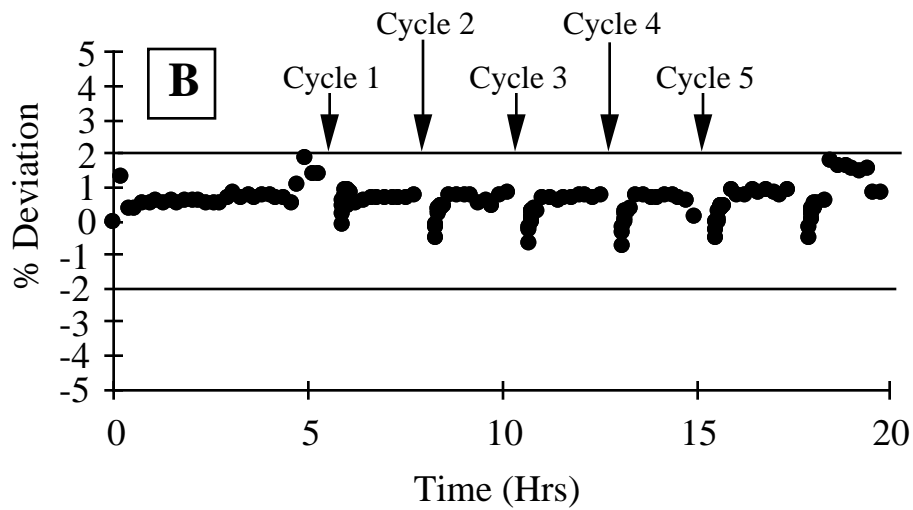
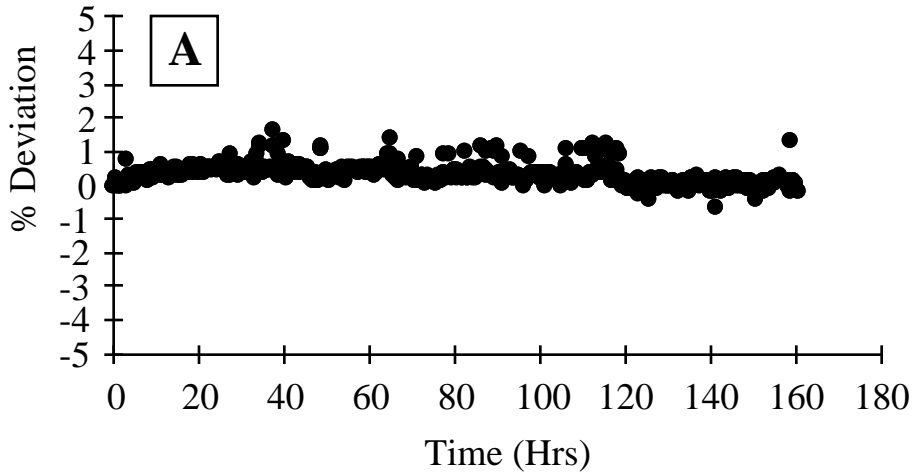
Figure 10) The peak anode current at which the response of candidate PMTs deviated by more than 2% from linearity at a gain of 50,000.

diode response value. The deviation from the fit as a function of PIN diode response is then calculated. A second linear fit is done for the region below the PIN diode response for which the deviation is a maximum. The deviations are then calculated with respect to the second least square fit values. The figure of merit is the peak anode current at which the deviation of the PMT response from the linear fit value exceeds  $\pm 2\%$ . All tubes were tested using the manufacturer's recommended voltage divider configuration for good linearity while maintaining adequate gain reach. Figure 9) shows the results from a typical linearity measurement. This PMT deviates from linearity by 2% at about 50 mA peak current. Figure 10) compares the linear response of samples of candidate PMTs. The peak current at which the response deviates from linearity by greater than 2%, when the tube is operating at a gain of  $5 \times 10^4$ , is histogrammed. The Thorn EMI tubes fall below our desired maximum peak current of 25 mA at this gain. As expected, the 8 stage Philips tubes displayed the best linear response since they must operate at the highest inter-dynode voltages to achieve a given gain. The 10 stage Philips and Hamamatsu PMTs had somewhat worse, though adequate, linearity.

## Stability

To evaluate the stability of candidate PMTs, three types of tests were performed: 1) stability versus time, 2) stability versus high voltage cycling, and 3) stability versus average anode current. Since stability measurements were very time consuming, PMTs were tested in a large test chamber in groups of approximately 20. They were excited by a laser system similar to that used for the linearity test. In addition to pulsed light from the laser system, light from a miniature tungsten lamp could be transmitted to the PMTs via 1mm clear plastic fibers to produce large steady state currents for test 3. Typical stability measurements proceeded as follows. At preset time intervals the ratio of the PMT to PIN diode<sup>16</sup> response, averaged over 500 flashes of the laser, was obtained. This "corrected response" used the PIN diode to remove the pulse to pulse variation in the light emitted from the laser, since the ratio of light delivered by the test system to the PIN diode and each PMT remains constant. Therefore, to the extent that the PIN diode is stable, the behavior in time of the corrected response of a PMT should reflect only the variations in its PMT response to pulsed light. The "Normalized Corrected Response" (NCR) is the corrected response at a given time divided by its initial value. It is this NCR which is monitored in the stability tests. Figure 11A) displays the results of a stability measurement for a PMT which was held at a constant voltage. For a tube to meet our specifications, its NCR was required to have less than a  $\pm 2\%$  deviation over any 48 hour period. Most PMTs that were tested easily satisfied this requirement.

During the setup of colliding beams at the Fermilab Tevatron, large beam losses may make it necessary to reduce or even turn off the high voltages of PMTs in the plug calorimeter, especially those servicing towers at the highest pseudorapidity ( $\eta$ ). It is therefore important to know how long the NCR takes to return to its nominal value when the high voltage is restored to its normal operating level after being reduced for some period. For our evaluations, we chose a cycle time of  $\sim 2$  hours at high voltage, followed by 30 minutes off. The figure of merit was the time required for the NCR to return to within  $\pm 3\%$  of its value as measured during the previous high voltage on period. The NCR shown in figure 11B) returns to within 1% of its nominal value in less than 20 minutes for the first cycle shown and less than 10 minutes for the second cycle shown. PMTs having NCRs that returned to within 3% of their nominal value within 10 minutes of restoring high voltage were deemed acceptable, and again there was not a problem for most tubes in



Figures 11. Phototube stability under three different conditions is shown for a typical Hamamatsu R4125. A) Long term stability with average anode currents of a few nA. The sporadic deviations from the trend were correlated with a PIN diode instability that has since been corrected. B) Gain recovery following interruptions in the tube high voltage. C) Gain shift correlated with a change in the average anode current. Two cycles are shown.

meeting this requirement.

The CDF plug calorimeter extends to  $|\eta|$  values of 3.6. The average anode current in PMTs servicing the highest  $\eta$  towers can reach as high as  $1 \mu\text{A}$  at the highest expected luminosity, due to the rate of low  $q^2$  events. The gain of PMTs can vary as a function of average anode current at the few percent level, due to a complicated process involving both electrostatic charging of the internal tube structure and surface chemical effects on the dynodes which modify their gains. The interplay of these effects leads to a variety of different, sometimes time dependent, behaviors of PMT response to pulsed light when a varying low level steady state background excitation is added, and we designed a test to study this effect. An example of one type of behavior observed under these conditions is shown in figure 11.C), which displays the NCR in the presence (solid circles) and absence (open circles) of steady state light from the tungsten lamp. In this case, the intensity of the steady-state light has been adjusted so that the anode current is  $745 \text{ nA}$ . The NCR of this PMT shows a downward shift of about 4% when the background light is turned on. Other PMTs showed upward shifts in their NCR. Our criterion for acceptance was that the shift be less than  $\pm 5\%$  for average anode currents up to  $1 \mu\text{A}$ . There were individual tubes from all types which failed or nearly failed this criterion, and no tube type displayed consistently superior behavior, (i.e. small shifts).

To summarize, although some tubes were found to fail the stability tests, there were not enough of any one type to merit disqualification of a vendor. Tests similar to those listed here will be used during acceptance testing of the production tubes to reject those tubes exhibiting poor performance.

### **Lifetime Test**

We measured the degradation of gain as a function of integrated anode charge for the R4125 and the XP1901 PMTs. In order to determine PMT aging characteristics under realistic conditions and still obtain results in a reasonable time period, we chose to run the tubes at average currents between  $3$  and  $5 \mu\text{A}$ . We were thus able to observe the effects of nearly  $100 \text{ C}$  of integrated anode charge in less than a year of testing. At the time we began this test, only the two tubes mentioned were candidates. During the test we made measurements of the average anode current, the response of the tube to a pulse signal superimposed on the background signal, and the gain of the PMT as determined using the "statistical method" previously outlined. The background light was provided by a tungsten lamp, coupled to the PMT through a  $1 \text{ mm}$  diameter light fiber approximately  $0.5$  meter long. The fiber was fixed to the front of a light mixer which in turn was held against the front face of the tube, so that the background light was spread over most of the PMT's active area. The pulsed light was provided by a red LED pulsed continuously at  $128 \text{ Hz}$ . The PMTs were operated at gains near  $1 \times 10^5$ . As can be seen in figure 12), the net decrease in response was about 12% for  $95 \text{ Coulombs}$  of integrated charge in the R4125 and 30% for  $80 \text{ Coulombs}$  of integrated charge in the XP1901. These results are confirmed when the PMT gains from before and after the test are compared. We also determined that after the test was completed the dark current in the tubes had not increased beyond  $2 \text{ nA}$ . These results indicate that both tube types would satisfy our requirements with regard to lifetime. Additional tests of the R4125 verified that other characteristics, such as linear response and quantum efficiency, were also unaffected by the large integrated charge.

### **Spontaneous Pulse Rate**

An important parameter of the tube assembly is its spontaneous pulse rate. The cathode and dynode of a PMT are continuously ejecting single electrons at a very

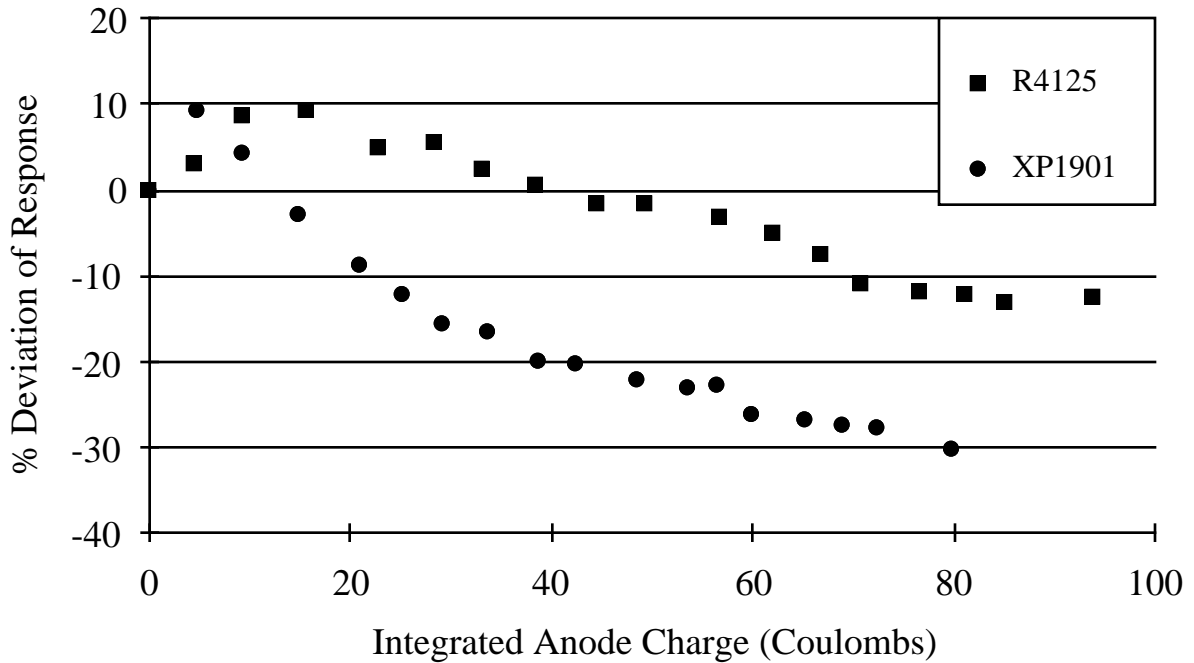


Figure 12) Change in response of an R4125 and an XP1901 PMT as a function of integrated anode charge.

low rate, and these are a component of the dark current. However, PMT systems can also produce much larger spontaneous signals that may be caused by flaws in the engineering of the electrostatic properties of the mechanical assembly that supports the tube. A prototype mechanical assembly was built to help determine whether our proposed assembly (shown in figure 13) was prone to this type of discharge. A 10.5 x 10.5 x 57 mm long acrylic light mixer was epoxied to the front face of the tube using Bicon BC 601 optical cement. Around the mixer is a 25 mm long plastic tubular extension with OD equal to that of the PMT. This extension is also epoxied to the face of the tube and around it is placed a copper foil which makes contact with and extends the manufacturer's electrostatic coating beyond the tube face. Heat-shrink tubing was applied over the length of the tube; the tubing was long enough to extend slightly beyond the end of the copper foil. The tube was then slid inside a "mu metal" shield which is held at ground potential and separated from the tube by two rubber O-rings. The free end of the light mixer is held in place by a plastic "light mixer guide", which has a set of locating pins to allow the assembly to interlock with the cookie containing the light fibers. In the final assembly, the mixer guide will be epoxied to the mu metal shield such that the mixer will be recessed 0.5 mm within the guide to insure uniform optical coupling of all fibers. The mu metal shield plus tube assembly is inserted into an iron pipe, which provides additional magnetic shielding. The shield is separated from the iron pipe with two O-rings. This assembly is held within the iron pipe by a threaded end cap which pushes on the base of the PMT via an O-ring. The O-ring makes the assembly light tight.

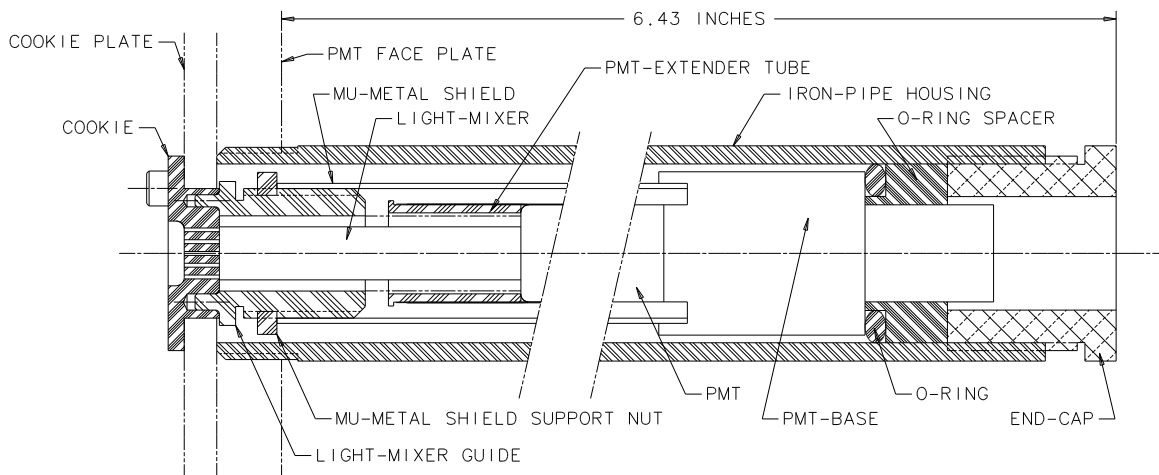


Figure 13) PMT mechanical assembly.

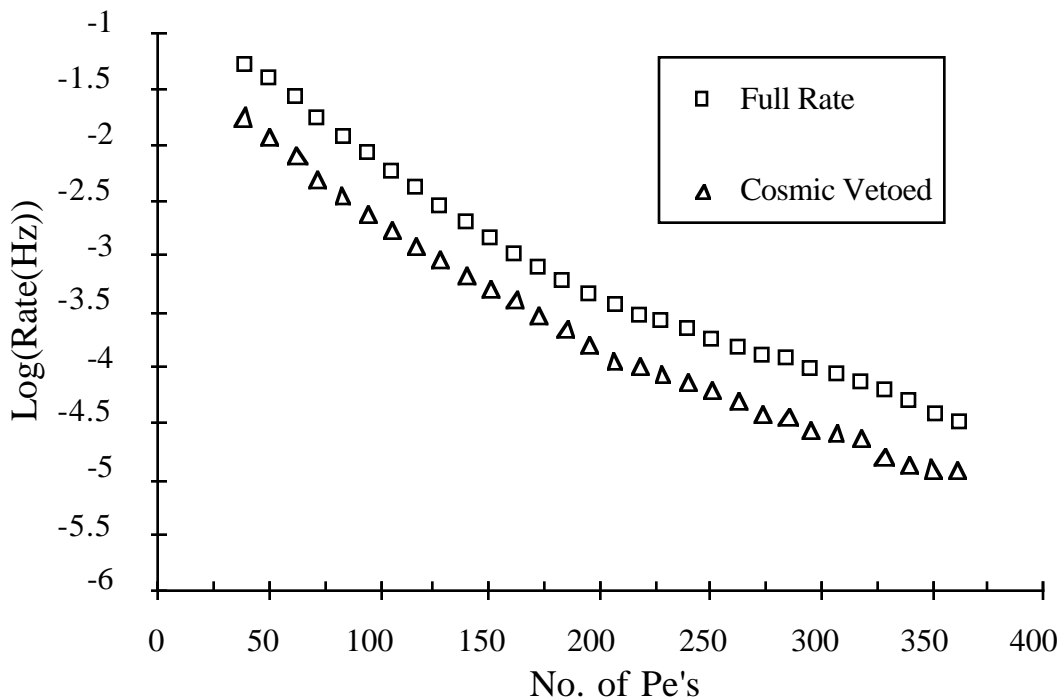


Figure 14) Spontaneous pulsing rate of a PMT housed within a prototype of the mechanical assembly as a function of number of photoelectrons. (A 1 GeV electron in the EM calorimeter is expected to produce about 350 pe's.)

The prototype assembly was placed between two scintillating paddles which were used to determine the rate of events produced by cosmic rays passing through the light mixer. The PMT was set to 1600 V, corresponding to a gain of  $7.3 \times 10^5$ . The output of the PMT was split, with one signal used to produce a gate signal for the ADC, and the other, after a suitable delay, sent to the ADC input. Since the spontaneous event rate was very low, the system had to be run for a number of days in order to gather a suitable statistical sample. A special module was built and was used to recalibrate the system periodically, to compensate for pedestal drifts due to temperature fluctuations in the room.

The result of this test was that the total event rate, for signals equivalent to 50 or more photoelectrons, was 0.051 Hz. Of this, at least 0.033 Hz was due to cosmic rays passing through the mixer. This is consistent with the rate calculated for the flux of cosmic ray muons through a cross sectional area equal to that of the mixer<sup>17</sup>. This leaves a rate of less than 0.018 Hz due to spontaneous pulsing of the PMT system. Figure 14 shows this rate for a run in which only cosmic rays making an angle of less than  $45^\circ$  with the vertical were vetoed. From this plot it can be seen that the spontaneous rate for signals greater than an equivalent 350 pe signal, which is the magnitude of the signal we expect from a 1 GeV electron in the EM calorimeter, is less than  $5 \times 10^{-5}$  Hz, corresponding to a total spurious rate, summed over all 960 plug calorimeter towers, of approximately 0.05 Hz. From similar calculations, we expect the spurious trigger rate from the hadron PMTs to be about 0.5 Hz for a  $P_t$  threshold of 6 GeV. This threshold is slightly lower than the current hadron trigger threshold in the CDF central calorimeter. Since the expected first level trigger rate in future running of the CDF detector will be thousands of Hz, we believe that these spontaneous discharge rates are acceptable. Additional tests using the final mechanical assembly design will be performed in the future.

## Conclusions

We have evaluated 5 different types of photomultiplier tubes which met our initial requirements with regard to size and sensitivity to the relevant spectrum of light from WLS fiber: the Burle C83012E, the Hamamatsu R4125, the Philips XP1901 and XP1981, and the Thorn EMI D919B. Of these, the Burle C83012E was not designed to operate at high peak pulse currents. The remaining tubes all met our gain and dark current requirements. The Hamamatsu R4125 appeared to have approximately 20% higher quantum efficiency than the other tubes and had a more uniform response over its active area. The Thorn EMI D919B tube had significantly less linear range than the R4125, the XP1901 or the XP1981. All four tube types performed comparably with respect to stability criteria. The CDF end plug upgrade project will use the R4125 PMT. The lifetime of the R4125 is acceptable, with the tube response degrading less than 15% for an integrated anode charge of nearly 100 C. This PMT, when coupled with our proposed mechanical assembly, has a very low spontaneous pulse rate and should not affect the detector event trigger rate significantly.

## Acknowledgments

We would like to acknowledge the many contributions to this work by the members of the Fermilab Detector and Accelerator Component R&D group: Irene Baum, Carol Diebold, Charles Hess, William Mumper, Jenny Reeves and Alan Rusy. We would also like to thank the Fermilab Physics Department, especially John Krider and Hogan Nguyen,

for the use of their PMT test facility and their help in conducting some of the tests reported in this paper.

This work was supported by the Department of Energy, the National Science Foundation, the Istituto Nazionale di Fisica Nucleare, Italy, the Ministry of Science, Culture and Education of Japan, the Natural Sciences and Engineering Research Council of Canada, and the A. P. Sloan Foundation.

---

<sup>1</sup>F. Abe et al., Nucl. Instr. and Meth. A271 (1982) 2015.

<sup>2</sup>Y. Fukui et al., Nucl. Instr. and Meth. A267 (1988) 280.

<sup>3</sup>G. Apollinari, P. de Barbaro, M. Mishina, CDF End Plug Calorimeter Upgrade Project, Proc. of the 4th Int. Conf. on Calorimetry in High Energy Physics, 1993.

S. Aota et al., Fermilab-Pub-94/240, submitted to Nucl. Instr. and Meth. A.

<sup>4</sup>Swan 486DB, Swan Technologies.

<sup>5</sup>Hewlett Packard HLMP-D105.

<sup>6</sup>Kiethly 486 picoammeter.

<sup>7</sup>Lecroy 2285 ADC module operated in 15 bit mode.

<sup>8</sup>LN 300 nitrogen laser, Laser Photonics, Inc.

<sup>9</sup>T. Devlin et al., Nucl. Instr. and Meth. A268 (1988) 24.

<sup>10</sup> $F_n$  is a function of the gain of the dynode stages and will increase as the gain decreases. For a discussion of this contribution to the pulse height resolution see, for example, appendix G of the Photomultiplier Handbook, copyright 1980 by Burle Technologies, Inc.

<sup>11</sup>J. Houston, Michigan State University, private communication.

<sup>12</sup>M. Akopyan et al., Nucl. Instr. and Meth. A330 (1993) 465.

<sup>13</sup>This measurement was done using a scanning device built by Michigan State University. For details, see B. H. Tannenbaum, *New Methods in Optical Fiber Preparation for Scintillating Tile Calorimetry*, Master's Thesis, Michigan State University, (1993).

<sup>14</sup>Esso Flyckt, private communication.

<sup>15</sup>Bicron 601 Optical Cement.

<sup>16</sup>Hamamatsu 1702-2.

<sup>17</sup>The cosmic ray event rate was estimated using values for fluxes published in the Review of Particle Properties.